Pergamon

Int. J. Heat Mass Transfer. Vol. 40, No. 14, pp. 3395–3406, 1997

Printed in Great Britain
0017–9310/97 $17.00+0.00

PII: S0017–9310(96)00374–2

Free and forced convection laminar film condensation on horizontal elliptical tubes

S. B. MEMORY
Department of Mechanical Engineering, University of Miami, Coral Gables, FL 33124, U.S.A.

and

V. H. ADAMS and P. J. MARTO
Department of Mechanical Engineering, Naval Postgraduate School, Monterey, CA 93943, U.S.A.

(*Received* 27 *December* 1995 *and in final form* 22 *October* 1996)

Abstract—Laminar film condensation on a horizontal elliptical tube in a pure saturated vapor was analyzed for conditions of free and forced convection. For free convection, a simple Nusselt type analysis was used. For forced convection, estimation of the interfacial shear stress was made in two ways: the first used an asymptotic value of the shear stress under conditions of infinite condensation rate and the second was based on simultaneously solving the two-phase vapor boundary-layer and condensate equations. Effects of surface tension and pressure gradient in the condensate film were also included. For free convection, an elliptical tube with the major axis vertical showed an improvement of nearly 11% in the mean heat-transfer coefficient when compared to a circular tube of equivalent surface area. For forced convection with the same approach velocity as for a circular tube, a small decrease ($\approx 2\%$) in the mean heat-transfer coefficient resulted. However, for the same pressure drop, heat transfer performance for an elliptical tube increased by up to 16%. © 1997 Elsevier Science Ltd.

1. INTRODUCTION

With the desire for smaller, less expensive shell and tube condensers, much effort has been devoted to improving the filmwise condensation mechanism on horizontal tubes. The majority of these studies has focused on passive enhancement techniques such as extended surfaces that improve heat transfer not only through an increase in the surface area to volume ratio, but also by utilizing surface tension to thin the condensate film. An alternative to this lies in the use of non-circular geometries, which serve to thin the condensate film not only through surface tension effects (manifested by the curvature of the surface), but also through an increased effect of gravity as a result of placing a larger proportion of the condensing surface in line with the vertical.

1.1. *Circular tubes*

For free convection laminar film condensation on vertical flat plates and circular tubes, the simple Nusselt [1] theory has been found in later more complete studies [2, 3] to be generally valid. For a circular tube, the mean heat-transfer coefficient can be calculated with good accuracy from:

$$\overline{Nu} = 0.728\left\{\frac{\rho_l^2 g h_{fg} d^3}{\mu_l \lambda_l (T_{sat} - T_{wall})}\right\}^{1/4}. \quad (1)$$

For forced convection laminar film condensation on a circular tube with vertical vapor downflow, Shekriladze and Gomelauri [4] obtained numerical solutions by assuming an approximate expression for the vapor shear stress on the condensate film. Rose [5] represented these results to within 0.4% by:

$$\overline{Nu} Re_{TP}^{-1/2} = \frac{0.9+0.728F^{1/2}}{(1+3.44F^{1/2}+F)^{1/4}} \quad (2)$$

where F is a dimensionless parameter that relates the relative importance of gravity to vapor shear on the motion of the condensate film. A better representation of vapor shear stress was made by Fujii *et al.* [6] and later corrected by Lee and Rose [7], where solution of the two-phase liquid and vapor boundary-layer equations was made with matching of the shear stress at the interface. They used an approximate integral solution of Truckenbrodt [8] to solve the momentum equation for flow over a tube with suction, slightly modified to agree more closely with the numerical solutions of Terril [9]. This analysis enables the point of vapor boundary-layer separation to be determined. Their results do not differ greatly from equation (2) except at low condensation rates.

Rose [5] additionally looked at the effects of pressure gradient on the condensate film using the simpler Shekriladze and Gomelauri [4] assumptions. He determined that for $(\rho_v U_\infty^2/\rho_l g d) > 1/8$, the rate of increase of the condensate film thickness becomes infinite at some angle φ_c on the rear of the tube and that solu-

NOMENCLATURE

a	ellipse semi-major axis length
b	ellipse semi-minor axis length
Bo	Bond number, $\rho_l g D_e^2/\sigma$
d	diameter of circular tube
D_e	effective diameter, equation (8)
$f_1(\varphi)$	gravity function, equation (9)
$f_2(\varphi)$	potential velocity function, equation (10)
$f_3(\varphi)$	pressure gradient function, equation (14)
$f_4(\varphi)$	surface tension function, equation (16)
F	$\mu_l D_e h_{fg} g/U_\infty^2 \lambda_l (T_{sat} - T_{wall})$
g	specific force of gravity
G	$(\lambda_l[T_{sat} - T_{wall}]/\mu_l h_{fg})(\rho_l \mu_l/\rho_v \mu_v)^{1/2}$
h_{fg}	specific enthalpy of evaporation
k	eccentricity, b/a
m	condensation mass flux rate
$\underline{Nu}$	local Nusselt number w.r.t. D_e
$\overline{Nu}$	mean Nusselt number w.r.t. D_e
P	$\rho_v h_{fg} \mu_l/\rho_l \lambda_l (T_{sat} - T_{wall})$
r,θ	cylindrical coordinates
$R(\varphi)$	radius of curvature, equation (6)
Re_{TP}	two-phase Reynolds number, $\rho_l U_\infty D_e/\mu_l$
Re_v	vapor Reynolds Number, $\rho_v U_\infty D_e/\mu_v$
T_{sat}	vapor saturation temperature
T_{wall}	tube wall temperature
u,v	condensate film velocity
U,V	vapor boundary layer velocity
U_φ	tangential velocity at edge of vapor boundary-layer
U_∞	vapor free stream velocity
x_1, y_1	ellipse Cartesian coordinates
x,y	curvilinear coordinates.

Greek symbols

α	orientation angle
δ	condensate film thickness
δ^*	dim. film thickness, $(\delta/D_e)Re_{TP}^{1/2}$
Δ	vapor boundary-layer thickness
Δ_1	vapor boundary-layer displacement thickness
Δ_2	vapor boundary-layer momentum thickness
φ	parametric angle
κ	pressure gradient parameter, equation (34)
κ_1	suction parameter, equation (34)
κ_a	parameter, equation (34)
λ	thermal conductivity
μ	dynamic viscosity
ρ	fluid density
σ	surface tension
τ	fluid shear force
$\chi(\varphi)$	defined by equation (7).

Subscripts/superscripts

δ	condensate film/vapor interface
l	condensate
v	vapor.

tions could not be obtained beyond this point. He found that the effect of pressure gradient was to generally increase the heat transfer over the forward half of the tube, but decrease it over the rear half. For cases where solutions were obtained over the whole tube $(\rho_v U_\infty^2/\rho_l g d) < 1/8$, inclusion of the pressure gradient led to a small decrease in the mean heat-transfer coefficient which was within 5% of equation (2) for all F. Krupiczka [10] examined the effects of surface tension due to curvature of the condensate film in a Nusselt type analysis on a circular tube and concluded that surface tension was only significant for small tubes or wires, where the rapidly changing film thickness could not be considered insignificant compared to the radius of the tube, i.e. violating one of Nusselt's assumptions.

1.2. *Non-circular tubes*

Limited analysis has been conducted on tubes of arbitrary non-circular cross-section i.e. non-elliptical. Dhir and Lienhard [11] applied a simple Nusselt type analysis to an arbitrary plane or axisymmetric body in which the component of gravity varied with streamwise length. They determined that Nusselt's expression for the mean heat-transfer coefficient (equation (1)) could be used if g were replaced by an effective gravity, g_{eff}, given by a simple expression similar to a weighted average gravity over the whole surface. Shklover and co-workers [12, 13] analyzed a horizontal tube having a surface profile such that the radius of curvature of the condensate always increased from the top to the bottom of the tube, thereby aligning more of the surface with the direction of gravity. By maximizing use of surface tension and gravity in this way, the condensate film was significantly thinned, resulting in a 20–30% increase in the mean heat-transfer coefficient compared to a circular tube of the same surface area. These numerical results were supported by limited experimental data. No work for forced convection on such tubes is known to the authors.

1.2.1. *Elliptical tubes—free convection.* An elliptical tube, with major axis aligned with the direction of gravity, should provide some of the advantages described above. From a design and fabrication standpoint, elliptical tubes provide a more practical solution than the complex tubes analyzed by Shklover and co-workers [12, 13]. To date, theoretical free convection film condensation studies on elliptical tubes have been analyzed using Nusselt type assumptions

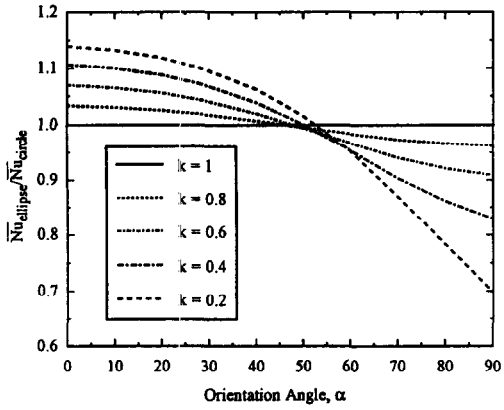

Fig. 1. Comparison of free convection mean Nusselt number for circular vs elliptical tube for varying eccentricity and orientation angle.

[14–18]. Cheng and Tao [14] approximated the surface by several circular arcs and determined that the mean heat-transfer coefficient was enhanced by 10–18% in the practical range of eccentricities† ($k = 0.3$–0.6) when compared to a circular tube with an equivalent surface area.

Wang *et al.* [15] considered condensation on elliptical tubes for which the major axis is aligned at some angle (the orientation angle, α) to the vertical. They concluded that a maximum mean heat-transfer coefficient was obtained for the condition at which the orientation angle $\alpha = 0°$, a result which was validated by limited experimental data on one elliptical tube with $k = 0.36$. Yang and Chen [16] noted that the mean heat-transfer coefficient had been incorrectly determined in the work of Wang *et al.* [15].‡ Correction of this error by the present authors is shown in Fig. 1 for varying eccentricity and orientation angle and resulted in a 5% decrease in the mean heat-transfer coefficients compared to those reported by Wang *et al.* [15]. However, for an elliptical tube with eccentricity $k = 0.36$, the theoretical mean heat-transfer coefficient for $\alpha = 0°$ is still 11.3% better than that for an equivalent surface circular tube. Furthermore, the elliptical tube outperformed the circular tube for orientation angles up to about 50°. This may have important implications in an elliptical tube bundle where approach velocities in some parts of the bundle may be offset from the vertical. Wang *et al.* [15] also conducted experimental work on an ellipse of eccentricity 0.36 using R-11. Subtracting the 5% correction to their numerical solutions mentioned above, better agreement with their experimental data was obtained.

Fieg and Roetzel [17] looked at the effect of axial inclination from the horizontal on the performance of elliptical tubes. They also found that for $k < 1$ (major axis in the vertical direction), the use of an elliptical surface increased the mean heat transfer compared to an equivalent surface circular tube. This increase was accentuated as the angle of inclination of the tube increased. Yang and Chen [16, 18] included the effects of surface tension on an elliptical tube due to curvature of the surface and variable wall temperature using a cosine distribution similar to that proposed by Memory and Rose [19] for a circular tube. In ref. [16], they concluded that surface tension had a negligible effect for an eccentricity§ $k > 0.8$. For $k < 0.8$, the effect of including surface tension was a small decrease in the mean heat-transfer coefficient, up to about 2% for $k \approx 0.4$. In ref. [18], they found that the variable wall temperature affected local values but not the mean value of the heat-transfer coefficient.

1.2.2. *Elliptical tubes—forced convection.*

Forced convection film condensation on an elliptical tube compared to a circular tube has the added potential advantage of a better streamlined shape resulting in improved vapor flow characteristics. Panday [20] developed an explicit numerical method for two-dimensional film condensation and applied it to the case of downward flowing vapor over elliptical tubes. Convection and inertia terms were included in the condensate film equations as well as pressure gradient and surface tension. Potential flow was assumed outside the vapor boundary-layer. The interfacial shear stress was estimated using an asymptotic expression similar to that used by Shekriladze and Gomelauri [4] for an infinite condensation rate. However, two errors related to the geometry of the ellipse were found in his analysis.‖ Correction of these errors by the present authors resulted in conclusions that are opposite to those reported by Panday [20]. At low vapor velocities where gravity is dominant, the mean heat-transfer coefficient was found to be larger than that of an equivalent surface area circular tube similar to that noted by other studies [14–16]. At high vapor velocities, the mean heat-transfer coefficient was found to be lower than an equivalent surface area circular tube due to a reduction in vapor drag (discussed later). The authors know of no other work (experimental or theoretical) for forced convection film condensation on an elliptical tube.

†The eccentricity of an ellipse is defined by $k = b/a$ where a and b are the radial distances in the vertical and horizontal directions, respectively. If the ellipse has its major axis vertical, then a and b are the semi-major and semi-minor axes, respectively.

‡In determining the average heat-transfer coefficient over the surface area, Wang *et al.* [15] took the radial distance of the ellipse, r, to be constant, whereas in reality, it varies with streamwise length.

§Note that Yang and Chen [16] use ellipticity (e) rather than eccentricity, defined as $e = \sqrt{a^2 - b^2}/a$ which varies from 0 for a circular tube to 1 for a vertical flat plate. Ellipticity is only defined for an ellipse with its major axis vertical where k and e are related by $k = \sqrt{1-e^2}$.

‖Referring to Fig. 2, the first error is a result of assuming that the differential streamwise length, dx is given by $r\,d\varphi$, which assumes that the radial distance from the centroid of the ellipse is constant over the interval of the parametric angle, φ. The second error is in the expression for r, which should be given by:

$$r = a\sqrt{\cos^2\varphi + k^2\sin^2\varphi}.$$

The present paper examines in more detail the effects of vapor shear, pressure gradient and surface tension for laminar film condensation on a single horizontal elliptical tube with its major axis aligned with gravity and/or with the free stream vapor flow. Interfacial shear is estimated using both the simple assumption of Shekriladze and Gomelauri [4] and the more complex model of Fujii *et al.* [6] for circular tubes. The latter also estimates the angle at which vapor boundary-layer separation occurs and the effect that it has on the mean heat-transfer coefficient.

2. THEORETICAL MODEL

2.1. *General considerations for an elliptical body*

Figure 2 shows an elliptical tube whose cross-section is oriented such that the major axis is aligned with the vertical. Functions relating the geometry of the ellipse are first given in a Cartesian coordinate system (x_1, y_1) whose center coincides with the centroid of the ellipse. These are then transformed into a cylindrical coordinate system (r, θ) where r is the radial distance from the centroid to a point on the ellipse surface at angle θ measured from the upper semi-major axis. However, the radial distance to a point on the ellipse surface is not constant with θ and the streamwise length, x, is, therefore, not proportional to θ as it would be for a circle. Consequently, when analyzing flow over a curved body shape other than a circle, it is more convenient to use curvilinear coordinates (rather than cylindrical coordinates), with x aligned along the streamwise elliptical wall surface and y along its normal with corresponding velocities u and v.

All three coordinate systems are functions of a parametric angle, φ, also measured from the upper semi-major axis. The parametric angle defines the elliptical surface such that the x_1 coordinate of a circle of radius b at angle φ translates to x_1 on the ellipse and the y_1 coordinate of a circle of radius a at angle φ translates to the y_1 coordinate on the ellipse. When $k = b/a = 1$ (circular tube), angle θ is equal to the parametric angle φ. The transformation equations are then given by:

$$x_1 = r\sin\theta = b\sin\varphi \tag{3}$$

$$y_1 = r\cos\theta = a\cos\varphi.$$

In Cartesian coordinates, the surface of the ellipse and radial distance, r, are given by:

$$(x_1/b)^2 + (y_1/a)^2 = 1 \tag{4}$$

$$r = \sqrt{x_1^2 + y_1^2} = a\sqrt{\cos^2\varphi + k^2\sin^2\varphi}. \tag{5}$$

The radius of curvature of the elliptical surface, $R(\varphi)$, is given by:

$$R(\varphi) = \frac{a}{k}[\sin^2\varphi + k^2\cos^2\varphi]^{3/2} \tag{6}$$

when $k = 1$ (circular tube), both r and $R(\varphi)$ are equal to a constant (a) as expected. To transform to curvilinear coordinates, consider point P on the ellipse shown in Fig. 2. Moving a small distance dx along the ellipse surface results in incremental changes of $d\theta$ and dr. The resulting relationship between x, r and θ is $(dx)^2 = (dr)^2 + (r\,d\theta)^2$. Combining this with equations (3) and (5) and differentiating where necessary gives expressions for dr and $d\theta$ (and hence dx) as a function of $d\varphi$:

$$dx = \chi(\varphi)d\varphi \tag{7}$$

where

$$\chi(\varphi) = a\sqrt{\frac{k^2 + \frac{1}{4}(k^2-1)^2\sin^2 2\varphi}{\cos^2\varphi + k^2\sin^2\varphi}}.$$

In formulating the problem, a characteristic length is used to non-dimensionalize the heat transfer parameters of the model. An effective diameter, D_e, is defined as the diameter of a circular tube which has the same surface area as the elliptical tube, given by:

$$D_e = \frac{2}{\pi}\int_0^{\pi}\chi(\varphi)\,d\varphi. \tag{8}$$

The component of gravity in the streamwise direction is tangent to the ellipse surface. A unit vector tangent to the surface is defined by the slope of the surface, dy_1/dx_1. The dot product of the tangent vector and the gravity vector yields the streamwise gravity component, g_x, given by:

$$g_x = gf_1(\varphi) \tag{9}$$

where

$$f_1(\varphi) = \frac{\sin\varphi}{\sqrt{\sin^2\varphi + k^2\cos^2\varphi}}$$

when $k = 1$ (circular tube), $f_1(\varphi) = \sin\varphi$. For forced vapor flow over the ellipse surface, the velocity of the vapor influences the condensate film thickness

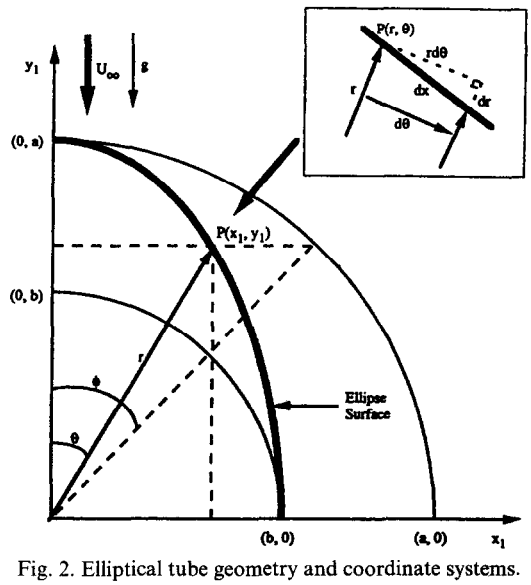

Fig. 2. Elliptical tube geometry and coordinate systems.

through the vapor shear at the interface. Assuming that both the film and vapor boundary-layer thicknesses are much smaller than the radius of curvature of the elliptical surface, the vapor velocity at the outer edge of the vapor boundary-layer for an ellipse with its major axis aligned with the vapor free stream velocity, U_φ, is given by potential theory:

$$U_\varphi = U_\infty f_2(\varphi) \tag{10}$$

where U_∞ is the oncoming vapor free stream velocity and $f_2(\varphi)$ is given by:

$$f_2(\varphi) = \frac{1+k}{\sqrt{1+k^2\cot^2\varphi}}$$

when $k = 1$ (circular tube), $f_2(\varphi) = 2\sin\varphi$.

2.2. *Asymptotic shear stress approximation*

Consider a pure saturated vapor at temperature T_{sat} flowing downward over a horizontal elliptical tube (oriented as in Fig. 2) with free stream velocity U_∞. The standard Nusselt [1] assumptions (including neglecting the inertia and convection terms) are used except that interfacial shear due to vapor flow is not negligible (represented by τ_δ) and the surface tension (due to curvature of the elliptical surface) and pressure gradient are included.

The interfacial shear is first approximated by the asymptotic expression assuming an infinite condensation rate, similar to that used by Shekriladze–Gomelauri [4]:

$$\tau_\delta = m(U_\varphi - u_\delta) \approx mU_\varphi. \tag{11}$$

Here, it is assumed that the film velocity at the interface is negligible compared to U_φ ($u_\delta \ll U_\varphi$). Subject only to the requirement that the boundary-layer (film) thickness be much smaller than the radius of curvature of the wall ($\delta \ll R(\varphi)$, White [21]), a momentum balance for an element in the condensate film in curvilinear coordinates, shown in Fig. 3(a), gives:

$$\mu_1 \frac{\partial^2 u}{\partial y^2} + \rho_1 g f_1(\varphi) - \frac{\mathrm{d}p}{\mathrm{d}x} = 0. \tag{12}$$

The total pressure gradient is a combination of that due to potential flow, p_φ and that due to surface tension, p_σ, given by:

$$\frac{\mathrm{d}p}{\mathrm{d}x} = \frac{\mathrm{d}p_\varphi}{\mathrm{d}x} + \frac{\mathrm{d}p_\sigma}{\mathrm{d}x}. \tag{13}$$

The pressure gradient due to potential flow is given by:

$$\frac{\mathrm{d}p_\varphi}{\mathrm{d}x} = -\rho_v U_\varphi \frac{\mathrm{d}U_\varphi}{\mathrm{d}x} = -\frac{\rho_v U_\infty^{\,2}}{2a} f_3(\varphi) \tag{14}$$

where

$$f_3(\varphi) = \frac{k^2(1+k)^2 \sin 2\varphi}{[\sin^2\varphi + k^2\cos^2\varphi]^2} \sqrt{\frac{\cos^2\varphi + k^2\sin^2\varphi}{k^2 + \frac{1}{4}(k^2-1)^2\sin^2 2\varphi}}$$

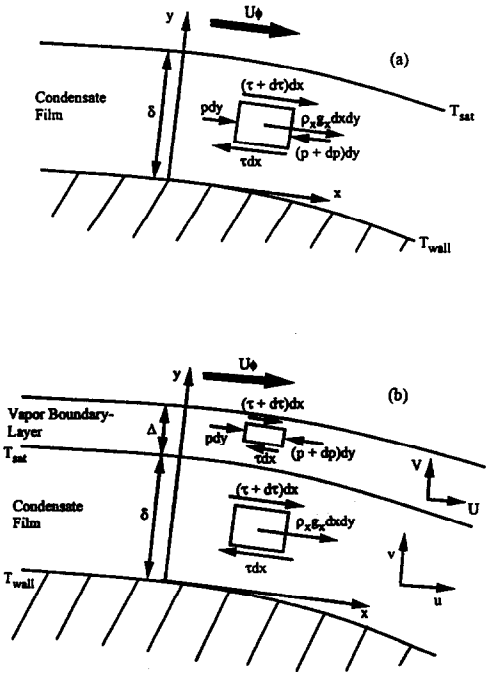

Fig. 3(a). Condensate film element for mixed convection with pressure gradient; (b) condensate film and vapor elements for mixed convection.

when $k = 1$ (circular tube), $f_3(\varphi) = 4\sin 2\varphi$. The pressure due to surface tension is given by:

$$p_\sigma = \frac{\sigma}{R(\varphi)}. \tag{15}$$

Assuming that $\delta \ll R(\varphi)$, the pressure gradient due to surface tension is then given by:

$$\frac{\mathrm{d}p_\sigma}{\mathrm{d}x} = -\frac{\sigma}{R(\varphi)^2}\frac{\mathrm{d}R(\varphi)}{\mathrm{d}x} = -\frac{3\sigma}{2a^2} f_4(\varphi) \tag{16}$$

where

$$f_4(\varphi) = \frac{k(1-k^2)\sin 2\varphi}{[\sin^2\varphi + k^2\cos^2\varphi]^{5/2}} \times \sqrt{\frac{\cos^2\varphi + k^2\sin^2\varphi}{k^2 + \frac{1}{4}(k^2-1)^2\sin^2 2\varphi}}$$

when $k = 1$ (circular tube), $f_4(\varphi)$ is zero since the curvature is constant for a circular tube. Combining equations (12)–(14) and (16) results in:

$$\mu_1 \frac{\partial^2 u}{\partial y^2} + \rho_1 g f_1(\varphi) + \frac{\rho_v U_\infty^{\,2}}{2a} f_3(\varphi) + \frac{3\sigma}{2a^2} f_4(\varphi) = 0 \tag{17}$$

subject to the following boundary conditions:

$$u_{y=0} = 0 \quad \text{and} \quad \mu_1 \left(\frac{\partial u}{\partial y}\right)_{y=\delta} = \tau_\delta = mU_\varphi. \tag{18}$$

A mass and energy balance for the condensate film gives:

$$m = \rho_l \frac{\mathrm{d}}{\mathrm{d}x}\left\{\int_0^\delta u\,\mathrm{d}y\right\} \tag{19}$$

$$= \frac{\rho_l}{\chi(\varphi)}\frac{\mathrm{d}}{\mathrm{d}\varphi}\left\{\int_0^\delta u\,\mathrm{d}y\right\} = \frac{\lambda_l(T_{sat}-T_{wall})}{\delta h_{fg}}$$

where δ is the local thickness of the condensate film and m is the condensation mass flux. Using equation (11), equation (17) can be solved for the condensate velocity (subject to the boundary conditions given by equation (18)) and combined with equation (19) to give the following equation for the dimensionless film thickness, δ^*:

$$\frac{1}{\delta^*} = \frac{D_e}{\chi(\varphi)}\frac{\mathrm{d}}{\mathrm{d}\varphi}\left\{\left[Ff_1(\varphi)+\frac{D_e}{2a}Pf_3(\varphi) + \tfrac{3}{2}\left(\frac{D_e}{a}\right)^2\frac{F}{Bo}f_4(\varphi)\right]\frac{\delta^{*3}}{3} + \tfrac{1}{2}f_2(\varphi)\delta^*\right\} \tag{20}$$

where δ^*, F, P and Bo are dimensionless parameters defined by:

$$\delta^* = \delta\sqrt{\frac{\rho_l U_\infty}{\mu_l D_e}} = \frac{\delta}{D_e}Re_{TP}^{1/2}$$

$$F = \frac{\mu_l D_e h_{fg} g}{U_\infty^2 \lambda_l (T_{sat}-T_{wall})}$$

$$P = \frac{\rho_v h_{fg}\mu_l}{\rho_l \lambda_l (T_{sat}-T_{wall})}$$

$$Bo = \frac{\rho_l g D_e^2}{\sigma}. \tag{21}$$

Due to the symmetry of the problem, the initial condition is given by:

$$\left(\frac{\mathrm{d}\delta^*}{\mathrm{d}\varphi}\right)_{\varphi=0} = 0. \tag{22}$$

With suitable values of the dimensionless parameters, equation (20) reduces to the analysis of Nusselt [1] for free convection alone, the analysis of Shekriladze and Gomelauri [4] for forced convection alone and the analysis of Rose [5] for forced convection incorporating pressure gradient. Equation (20) was solved using a fifth-order Adams method predictor–corrector algorithm developed from Crandall [22]. The mean heat-transfer coefficient, given in dimensionless form, was then determined from:

$$\overline{Nu}Re_{TP}^{-1/2} = \frac{2}{\pi}\int_0^\pi \frac{1}{\delta^*}\chi(\varphi)\,\mathrm{d}\varphi. \tag{23}$$

As in the study of pressure gradient by Rose [5], there is a condition for which $\mathrm{d}\delta^*/\mathrm{d}\varphi$ becomes infinite at some critical angle, φ_c. Differentiating equation (20) results in a first-order ordinary differential equation for δ^*. Solving for $\mathrm{d}\delta^*/\mathrm{d}\varphi \to \infty$ yields:

$$\left[2Ff_1(\varphi)+\frac{D_e}{a}Pf_3(\varphi)+3\left(\frac{D_e}{a}\right)^2\frac{F}{Bo}f_4(\varphi)\right]\delta^{*3} + f_2(\varphi)\delta^* = 0 \tag{24}$$

This condition determines φ_c and is always satisfied at an angle which occurs before the condition for condensate film separation ($\mathrm{d}u/\mathrm{d}\varphi = 0$ at $y = 0$). With surface tension neglected, equation (24) reduces to that given by Rose [5] for a circular tube ($k = 1$). It should be noted that vapor boundary-layer separation is not predicted by the asymptotic shear stress approximation since the interfacial shear is based on potential flow outside the vapor boundary-layer which is always positive.

2.3. *Two-phase boundary–layer approximation*

As mentioned earlier, the interfacial shear stress expression of Shekriladze and Gomelauri [4] was modified by Fujii *et al.* [6] for a circular tube by simultaneously solving the boundary-layer equations for the condensate film and vapor, together with compatibility of interfacial shear at the vapor/condensate interface. This method is now applied to an elliptical tube oriented as in Fig. 2. Since this analysis is more complex, pressure gradient and surface tension effects have been neglected—all other assumptions are the same as above. Elements of the condensate film and vapor are shown in Fig. 3(b). The equations of momentum, energy and continuity for the condensate film are derived as before (except that the momentum equation has no pressure gradient or surface tension terms), giving the following ordinary differential equation for δ^*:

$$\frac{1}{\delta^*} = \frac{D_e}{\chi(\varphi)}\frac{\mathrm{d}}{\mathrm{d}\varphi}\left\{Ff_1(\varphi)\frac{\delta^{*3}}{3}+\frac{\bar{\tau}_\delta\delta^{*2}}{4G}\right\} \tag{25}$$

where G and $\bar{\tau}_\delta$ are dimensionless parameters given by:

$$G = \frac{\lambda_l(T_{sat}-T_{wall})}{\mu_l h_{fg}}\sqrt{\frac{\rho_l\mu_l}{\rho_v\mu_v}} \quad \text{and} \quad \bar{\tau}_\delta = \frac{2\tau_\delta\sqrt{Re_v}}{\rho_v U_\infty^2}.$$

The governing equations for the vapor boundary-layer are given by:

$$\frac{\partial U}{\partial x}+\frac{\partial V}{\partial y} = 0 \quad \text{(continuity)}$$

$$U\frac{\partial U}{\partial x}+V\frac{\partial U}{\partial y} = U_\varphi\frac{\mathrm{d}U_\varphi}{\mathrm{d}x}+\left(\frac{\mu_v}{\rho_v}\right)\frac{\partial^2 U}{\partial y^2}. \quad \text{(momentum)} \tag{26}$$

The system of equations is subject to the following boundary conditions at the wall, vapor/condensate interface and outer edge of the vapor boundary-layer, respectively:

$$y = 0: \quad u = v = 0$$

$$y = \delta: \quad u = U \approx 0; \quad \mu_l \left(\frac{\partial u}{\partial y}\right) = \mu_v \left(\frac{\partial U}{\partial y}\right) = \tau_\delta;$$

$$-\rho_v V_\delta = \frac{\lambda_l (T_{sat} - T_{wall})}{h_{fg}\delta}$$

$$y = \delta + \Delta: \quad U = U_\varphi; \quad \left(\frac{\partial U}{\partial y}\right) = 0. \tag{27}$$

Integrating equations (26) over the vapor boundary-layer thickness, Δ, and eliminating V yields:

$$\frac{1}{U_\varphi^2}\frac{d}{dx}\{U_\varphi^2 \Delta_2\} + \frac{\Delta_1}{U_\varphi}\frac{dU_\varphi}{dx} = \frac{V_\delta}{U_\varphi} + \frac{\tau_\delta}{\rho_v U_\varphi^2} \tag{28}$$

where Δ_1 and Δ_2 are the displacement and momentum thicknesses given, respectively, by:

$$\Delta_1 = \int_\delta^{\delta+\Delta} \left(1 - \frac{U}{U_\varphi}\right) dy \tag{29}$$

$$\Delta_2 = \int_\delta^{\delta+\Delta} \frac{U}{U_\varphi}\left(1 - \frac{U}{U_\varphi}\right) dy.$$

Truckenbrodt [8] developed a simplified approximation to the solution of equation (25). Using his approach, equation (28) reduces to the following dimensionless ordinary differential equation:

$$\frac{dZ}{d\varphi} = \frac{1}{\bar{U}_\varphi}\frac{\chi(\varphi)}{D_e}\left\{0.441[1 + 2\bar{V}_\delta\sqrt{Re_v Z}] - \frac{6D_e}{\chi(\varphi)}\frac{d\bar{U}_\varphi}{d\varphi} Z\right\} \tag{30}$$

where

$$\bar{U}_\varphi = \frac{U_\varphi}{U_\infty}, \quad \bar{V}_\delta = \frac{V_\delta}{U_\infty}, \quad Z = Re_v\left(\frac{\Delta_2}{D_e}\right)^2. \tag{31}$$

The initial condition for equation (30) is that $dZ/d\varphi = 0$ at $\varphi = 0$. Compatibility at the vapor/condensate interface requires that:

$$-\bar{V}_\delta\sqrt{Re_v} = \frac{G}{\delta^*} \tag{32}$$

for the vapor boundary–layer and:

$$\bar{\tau}_\delta = \frac{2\tau_\delta\sqrt{Re_v}}{\rho_v U_\infty^2} = 6.44\bar{U}_\varphi\frac{\sqrt{\kappa_a(\kappa_a + \kappa)}}{\sqrt{Z}} \tag{33}$$

for the condensate film, where

$$\kappa_a = 0.0682 + 0.174\kappa_1; \quad \kappa_1 = \frac{G}{\delta^*}\sqrt{Z};$$

$$\kappa = \frac{D_e}{\chi(\varphi)}\frac{d\bar{U}_\varphi}{d\varphi} Z. \tag{34}$$

With suitable values of the dimensionless parameters, equation (25) reduces to the analysis of Fujii *et al.* [6] for forced convection, as corrected by Lee and Rose [7]. δ^* is obtained by differentiating equation (25) and solving simultaneously with the differential equation for the vapor boundary-layer (equation (30)) subject to the compatibility equations (33) and (34). Due to the stiffness of the problem, an algorithm based on Gear's stiff method [23] was used. Once δ^* has been determined, the mean heat-transfer coefficient is calculated as before from equation (23). Vapor boundary-layer separation is assumed to occur at $\tau_\delta \leqslant 0$. Downstream of the separation point, the heat-transfer coefficient is assumed to be given by Nusselt [1] theory.

3. DISCUSSION OF RESULTS

When comparing local values of film thickness and heat-transfer coefficient, a dimensionless streamwise length, x^* is used, defined as the ratio of the streamwise length, x, to the half perimeter length ($x^* = 2x/\pi D_e$). Its use provides a direct comparison between elliptical and circular tubes as it represents an equivalent surface area. The effective diameter of an equivalent surface area circular tube is given by equation (8).

3.1. *Free convection* ($F \to \infty$, *no effect of vapor shear*)

When comparing mean heat transfer coefficients for an elliptical tube with those of a circular tube, equivalent surface areas have been used. Dimensionless mean heat-transfer coefficients have been obtained over a wide range of eccentricity (k) and are shown in Fig. 4; good agreement with earlier elliptical tube studies [15, 16] is obtained. Results for the special cases of a circular tube ($k = 1$) and a vertical flat plate ($k \to 0$, $L = 2a$), agree well with those of Nusselt [1]. For a horizontal flat plate ($k \to \infty$), the heat-transfer

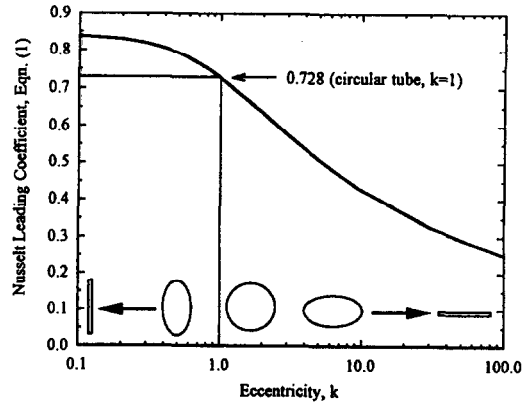

Fig. 4. Effect of eccentricity on mean Nusselt number for free convection.

†For a finite horizontal flat plate, condensate will flow over the edges yielding finite heat transfer [24].

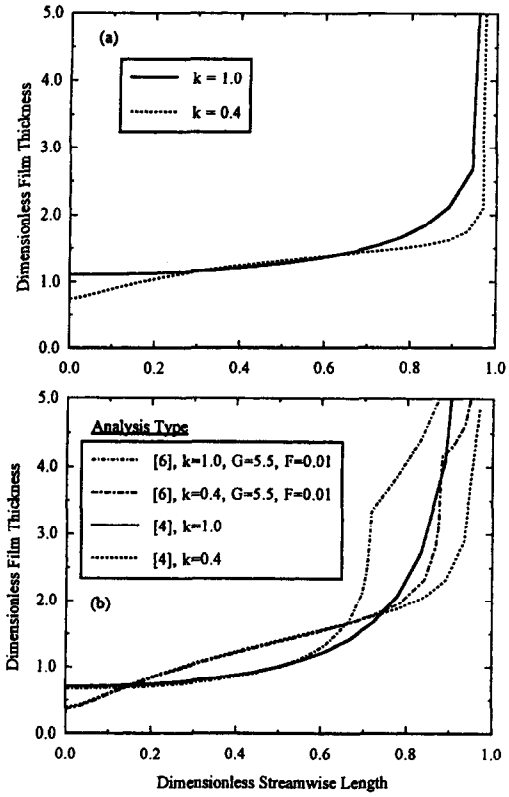

Fig. 5. Effect of eccentricity on local film thickness: (a) free convection; (b) forced convection (using shear stress models from refs. [4] and [6]).

coefficient approaches zero as the film thickness becomes infinite.† For a practical manufacturing range of eccentricity ($0.4 < k < 0.6$), it can be seen that the effect of placing more of the elliptical tube surface in the direction of gravity is to increase the mean heat-transfer coefficient by 7% at $k = 0.6$ increasing to nearly 11% at $k = 0.4$. The reasons for this are due to the variations in local dimensionless film thickness as discussed below.

For free convection ($F \to \infty$), Fig. 5(a) shows values of local dimensionless film thickness vs dimensionless streamwise length for two values of eccentricity, $k = 1$ (circular tube) and $k = 0.4$ (a practical elliptical tube). The effect of gravity thins the condensate film over the front and rear portions of the elliptical tube compared with the circular tube, but is slightly thicker in the middle region. The thickness of the film is determined by a balance of two effects: the condensation rate and the condensate film velocity. At the top of the elliptical tube, the increased effect of gravity (compared with the circular tube) increases the condensate velocity, resulting in a thinner film. The thinner film, however, results in a higher condensation rate, which tends to thicken the film further downstream. With no difference in the gravity component at 90°, the film for the elliptical tube is, therefore, thicker in this middle region. Over the rear half of the elliptical tube, the reduced condensation rate (due to the now thicker film) and the larger gravity component results in a slower thickening of the condensate film compared with the circular tube.

3.2. *Forced convection* ($F \to 0$, *no effect of gravity*)

With vapor shear, the streamlined shape of an elliptical tube causes higher vapor velocities over the front and rear portions, but a lower vapor velocity over the middle region. For "pure" forced convection ($F \to 0$), the effects of vapor shear on the dimensionless film thickness can be seen in Fig. 5(b) for eccentricities of 1.0 (circular tube) and 0.4. For the elliptical tube, the larger shear stress at the top of the tube due to the higher vapor velocity (when compared to a circular tube) results in a thinner condensate film. This causes a higher condensation rate which, when combined with the lower relative vapor velocity over the middle section of the tube, leads to a thicker condensate film in this region. Over the rear portion of the elliptical tube, the now lower condensation rate combined with the higher vapor shear once again results in a thinner film than with a circular tube.

Figure 5(b) shows solutions using both the asymptotic (Shekriladze-Gomelauri [4]) and boundary-layer (Fujii *et al.* [6]) shear stress approximations. Both give very similar solutions over the front half of both tubes, but vary considerably over the rear half with the latter clearly showing the points at which the boundary-layer separates (discussed in more detail below). No separation is seen with the asymptotic (infinite condensation rate) shear stress approximation, as expected. The effect of these local variations in film thickness is to reduce the mean heat-transfer coefficient for the elliptical tube by between 1–2% for practical values of k (0.4–0.6) when compared to a circular tube (see Fig. 6(a) below). From studies of single phase flow over an elliptical tube, the drag force has been found to be reduced when compared to a circular tube [25]. This reduced interfacial drag results in a thicker condensate film for the ellipse and accounts for this small decrease in heat transfer compared to a circular tube for the same free stream velocity.

3.3. *Combined free and forced convection*

3.3.1. *Asymptotic shear stress approximation* [4]. Figure 6(a) shows the effect of eccentricity on the ratio of the mean heat-transfer coefficient for an elliptical tube and a circular tube of the same surface area: both free ($F \to \infty$) and forced convection ($F \to 0$) using the asymptotic shear stress approximation [4] are shown. For the case of a circular tube ($k = 1$), the solutions for the mean heat-transfer coefficient are within 0.4% of equation (2) given by Rose [5]. As $F \to \infty$, the free convection solutions given in Fig. 4 are approached, resulting in the small increase in the mean heat transfer coefficient of nearly 11% as eccentricity decreases from 1.0 to 0.4. If tubes of eccentricity equal to 0.2 could be feasibly manufactured, then increases of nearly 14% are predicted. As $F \to 0$, the elliptical tube

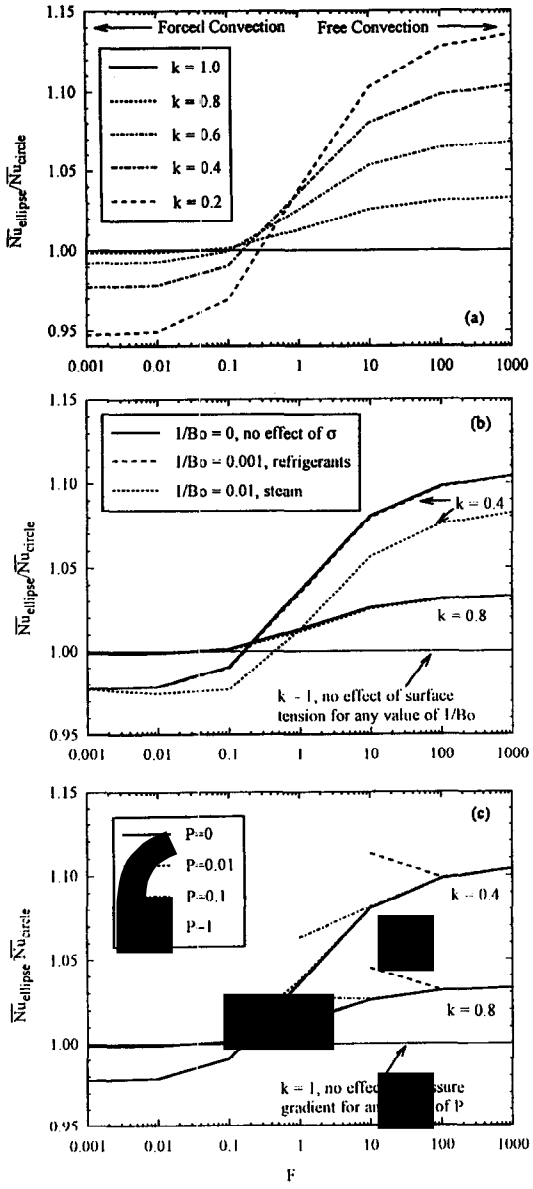

Fig. 6. Effect of varying eccentricity, surface tension and pressure gradient on the mean Nusselt number for free and forced convection (using shear stress model from ref. [4]: (a) k; (b) $1/Bo$; (c) P.

shows a small decrease in the mean heat transfer coefficient of around 2% as eccentricity decreases from 1.0 to 0.4. The reasons for this small decrease were given above in Fig. 5(b).

3.3.2. *Effect of surface tension.* The effect of surface tension has been studied separately using only the asymptotic shear stress approximation [4]. Only those cases for which a solution could be obtained over the whole tube are presented. Surface tension causes a favorable pressure gradient over the front half of an elliptical tube and an adverse pressure gradient over the rear half. The severity of the pressure gradient is localized to small regions at the top and bottom of the elliptical tube where the change in surface curvature is most severe. Consequently, it is expected that effects of surface tension are going to increase as k decreases.

Figure 6(b) shows the effect of surface tension on the mean heat-transfer coefficient for both free and forced convection for ellipses of eccentricity 0.4 and 0.8 when compared to a circular tube of similar surface area ($k = 1$). The reciprocal of the Bond number, $1/Bo$, gives the relative effect of surface tension to inertia and is typically around 0.01 for steam and 0.001 for refrigerants. It can be seen that the influence of surface tension is almost negligible for a highly wetting fluid such as refrigerant (lines cannot be distinguished). Also, as eccentricity decreases, the line for $1/Bo = 0.01$ lies below that for $1/Bo = 0$ over the whole range of F, indicating that inclusion of surface tension leads to a small decrease in the mean heat-transfer coefficient for steam for both free ($\approx 2\%$) and forced ($<0.5\%$) convection. This suggests that any thinning of the condensate film over the top half of the tube is more than offset by a thickening over the lower half. Decreasing k accentuates these decreases, which are more significant in the free convection region (where surface tension can dominate gravity) than in the forced convection region where film thickness remains dominated by vapor shear.

3.3.3. *Effect of pressure gradient.*

The effect of pressure gradient has also been studied separately using the asymptotic shear stress approximation [4]. Again, only those cases for which a solution could be obtained for the whole tube are presented. The pressure gradient included in the momentum equation of the condensate film (equation (12)) is assumed to be due to the pressure gradient impressed on the condensate film by vapor potential flow. As with surface tension, there is a favorable pressure gradient over the front half of an elliptical tube and an adverse pressure gradient over the lower half. The effect of decreasing eccentricity ($k < 1$) is to push the points of maximum favorable and adverse pressure gradient to the front and rear of the tube, respectively. This delays the point at which the condensate film thickness becomes infinite and is a result of the better streamlined shape of the elliptical tube.

With pressure gradient included, solutions agree with the results of Rose [5] for a circular tube ($k = 1$), giving the same 5% decrease in the mean heat-transfer coefficient over the whole range of F when compared to equation (2). Using practical values of the dimensionless parameter P ($0.01 < P < 1$), Fig. 6(c) shows the effect of including pressure gradient on the mean heat-transfer coefficient for free and forced convection for ellipses of eccentricity 0.4 and 0.8 when compared to a circular tube ($k = 1$) of similar surface area. For values of F for which solutions could be obtained for the whole tube, increasing P has the effect of increasing the mean heat-transfer coefficient for the ellipse when compared to the circular tube. This is a result of the more favorable potential velocity distribution around the ellipse. These increases are more significant

in the free convection region than in the forced convection region where film thickness remains dominated by vapor shear (as with surface tension). It can be seen from Fig. 6(c) that complete solutions could only be obtained for certain values of P and F, given by:

$$P \leqslant \frac{a}{D_e}\left(\frac{k}{1+k}\right)^2 F \tag{35}$$

when $k = 1$ and $D_e = 2a$, equation (35) reduces to that given by Rose [5] for a circular tube.

3.3.4. *Effect of vapor pressure drop.*

It has been shown above that for an elliptical tube with its major axis vertical, the mean heat-transfer coefficient is lower than an equivalent surface circular tube for a fixed vertical vapor downflow (Fig. 6(a), low F). However, for a fixed vapor pressure drop, the approach velocity for an elliptical tube can be significantly higher than that for a circular tube. Sample calculations using steam ($T_{sat} = 60°C$) condensing on a horizontal tube with $T_{wall} = 40°C$ have shown that for a fixed pressure drop, the approach velocities for a circular and an elliptical tube with $k = 0.5$ are 25 and 35 m/s, respectively.† This gives a 16% higher mean heat transfer for an elliptical tube over a circular tube when using the asymptotic shear stress approximation [4].

3.3.5. *Two-phase boundary-layer shear stress approximation* [6].

Solution of the two-phase boundary-layer equations with matched shear stress at the interface allows the vapor boundary-layer separation point and its effect on local and mean heat transfer rates to be determined. For a circular tube ($k = 1$), the present solutions agree closely with the results of Fujii *et al.* [6] as corrected by Lee and Rose [7]. Local film thickness has already been shown in Fig. 5(b) for a circular and elliptical tube ($k = 0.4$) for forced convection ($F \to 0$) and high values of G, a dimensionless parameter which is proportional to condensation rate.‡ Both tubes exhibit a rapidly thickening condensate film as the separation point is approached due to the reduced shear effect ($\tau_\delta \to 0$). For the elliptical tube, however, the figure clearly indicates a delay in vapor boundary-layer separation due to the better streamlined shape. This leads to a thinner film and a higher overall heat transfer rate for the elliptical tube, as mentioned earlier.

In reality, the overall heat transfer rate is a complicated function of gravity ($F \to \infty$), vapor shear ($F \to 0$) and delay of vapor boundary-layer separation

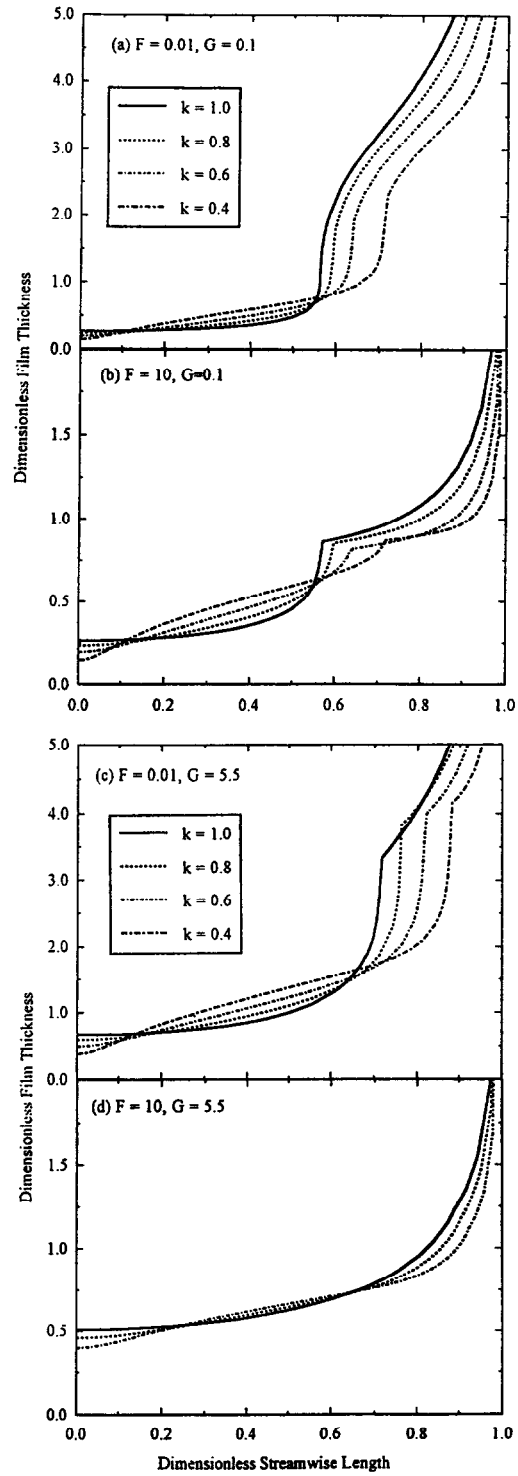

Fig. 7. Effect of eccentricity on local condensate film thickness (using shear stress model from ref. [6]: (a) $F = 0.01$, $G = 0.1$; (b) $F = 10$, $G = 0.1$; (c) $F = 0.01$, $G = 5.5$; (d) $F = 10$, $G = 5.5$.

($G \to \infty$, $F \to \infty$). Figures 7 and 8 show how these three phenomena affect local film thickness and local heat-transfer coefficients for varying eccentricity using four extreme practical combinations of F and G

†In the absence of two-phase drag coefficients, single-phase drag coefficients of 1.2 and 0.6 have been used, respectively, for a cylinder and an elliptical tube with $k = 0.5$ (taken from White [25]).

‡Practical ranges of G are 0.1 to about 2.5 for refrigerants and 0.3 to about 5.5 for steam.

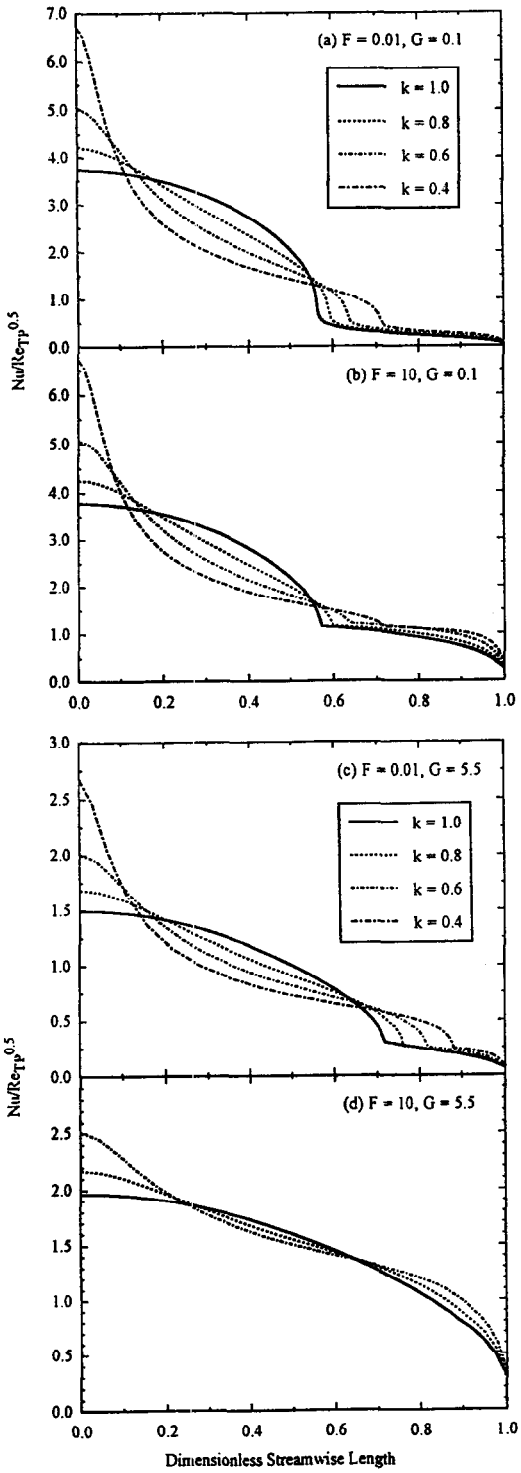

Fig. 8. Effect of eccentricity on local heat transfer coefficient (using shear stress model from ref. [6]): (a) $F = 0.01$, $G = 0.1$; (b) $F = 10$, $G = 0.1$; (c) $F = 0.01$, $G = 5.5$; (d) $F = 10$, $G = 5.5$.

$(0.01 < F < 10; 0.1 < G < 5.5)$. In all four cases, the delay in vapor boundary-layer separation with decreasing k is clear. For low F and G, the separation point occurs relatively early and close to the position

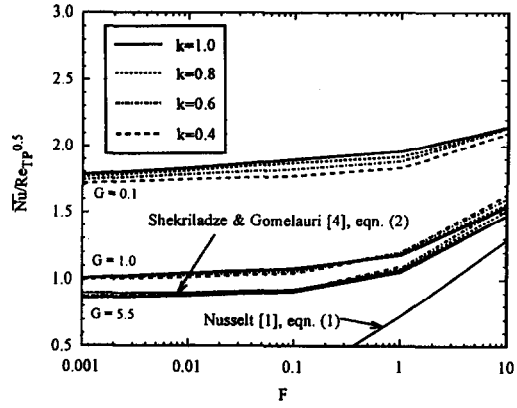

Fig. 9. Effect of eccentricity and condensation rate on mean Nusselt number for free and forced convection (using shear stress model from [6]).

obtained for single phase separation without suction. As F and G increase (decreasing U_∞ and increasing condensation rate (suction), respectively), vapor boundary-layer separation is further delayed and is virtually eliminated at high values of both. Note that in Figs 7(b,c) and 8(b,c), the point of separation seems to cause a much more abrupt change in the film thickness. This is because, downstream of the separation point, the heat-transfer coefficient is assumed to be given by Nusselt [1] theory.

Figure 9 shows how the three phenomena above influence the mean heat-transfer coefficient for varying eccentricity. For free convection (high F), all solutions tend to converge to the Nusselt [1] model. For high condensation rates ($G = 5.5$), the two-phase shear stress approximation of Fujii *et al.* [6] agrees closely with the asymptotic shear stress approximation of Shekriladze and Gomelauri [4] as expected. For all practical values of G, the effect of eccentricity is similar to that discussed in Fig. 6(a) above, with an increase in mean heat transfer (compared to a circular tube) at high F and a small decrease at low F. However, as G increases, the cross-over point from increase to decrease (i.e. changing from a gravity dominated flow to a shear dominated flow) occurs at ever decreasing values of F (higher U_∞). This appears to be due to the effects of vapor boundary-layer separation. At high F and G, the separation point is delayed at different rates depending on eccentricity, increasing as k decreases. As F decreases, the separation point moves forward only slightly due to the very high suction. The delayed separation for the elliptical tube results in a higher mean heat-transfer coefficient and thus, at high G, the flow is gravity dominated for a wide range of F. At low F and G, separation occurs close to that for single phase dry friction. As F increases, there is little change in this separation point. The reduced drag for the elliptical tube in the region before separation causes a reduction in the mean heat-transfer coefficient and thus, at low G, the flow is shear dominated for a wide range of F.

4. CONCLUSIONS

Analyses of laminar film condensation on a horizontal elliptical tube have been conducted under conditions of free and forced convection using both asymptotic and two-phase boundary-layer interfacial shear stress approximations. For the asymptotic shear stress approximation, effects of surface tension and pressure gradient have also been independently studied. Results have been compared to a circular tube of an equivalent surface area.

For free convection, gravity provides a small increase in the mean heat transfer by placing more of the elliptical tube surface in the direction of gravity. For forced convection at a given free stream velocity, both shear stress approximations indicate a small decrease in mean heat transfer due to a reduction in the interfacial shear as a result of the better streamlined shape of the elliptical tube. However, for a given pressure drop across each tube, the higher allowable vapor approach velocity for the elliptical tube results in an increase in the mean heat-transfer coefficient for both shear stress approximations. Some enhancement may also be due to a delay in vapor boundary-layer separation that occurs with the better streamlined body. Surface tension and pressure gradient effects on the mean heat-transfer coefficient are small, leading to a small decrease and a small increase for all F, respectively.

REFERENCES

1. Nusselt, W., Die Oberflächenkondensation des Wasserdampfes. *Z.V.D.I.*, 1916, **60**, 569–575.
2. Sparrow, E. M. and Gregg, J. L., A boundary layer treatment of laminar film condensation. *Journal of Heat Transfer*, 1959, **81C**, 13–18.
3. Sparrow, E. M. and Gregg, J. L., Laminar condensation heat transfer on a horizontal cylinder. *Journal of Heat Transfer*, 1959, **81C**, 291–296.
4. Shekriladze, I. G. and Gomelauri, V. I., Theoretical study of laminar film condensation of flowing vapour. *International Journal of Heat and Mass Transfer*, 1966, **9**, 581–591.
5. Rose, J. W., Effect of pressure gradient in forced convection film condensation on a horizontal tube. *International Journal of Heat and Mass Transfer*, 1984, **27**, 39–47.
6. Fujii, T., Honda, H. and Oda, K., Condensation of steam on a horizontal tube—the influence of oncoming velocity and thermal condition at the tube wall. In *Condensation Heat Transfer*. ASME, New York, 1979, pp. 35–43.
7. Lee, W. C. and Rose, J. W., Film condensation on a horizontal tube—effect of vapour velocity. *Proceedings of the 7th Int. Heat Transfer Conference*, Vol. 5, Munich, 1982, pp. 101–106.
8. Truckenbrodt, E., Ein einfaches Näherungsverfahren zum Berechnen der laminaren Reibungsverfahren mit Absaugung. *Forschung*, 1956, **22**, 147–157.
9. Terril, R. M., Laminar boundary-layer flow near separation with and without suction. *Philosophical Transactions of the Royal Society of London—Series A*, 1960, **253**, 55–100.
10. Krupiczka, R., Effect of surface tension on laminar film condensation on a horizontal cylinder. *Chemical Engineering Process*, 1985, **19**, 199–203.
11. Dhir, V. and Lienhard, J., Laminar film condensation on plane and axisymmetric bodies in non-uniform gravity. *Journal of Heat Transfer*, 1971, **93**, 97–100.
12. Shklover, G. G., Semenov, V. P., Pryakhin, V. V. and Usachev, A. M., Heat transfer with steam condensing on a horizontal tube with a profile of variable curvature. *Thermal Engineering*, 1985, **32**, 125–127.
13. Semenov, V. P., Shklover, G. G., Usachev, A. M. and Semenova, T. P., Enhancement of heat transfer in condensation of steam on a horizontal noncircular pipe. *Heat Transfer—Soviet Research*, 1990, **22**(1), 15–20.
14. Cheng, S. and Tao, J., Study of condensation heat transfer for elliptical pipes in stationary saturated vapor. *Proceedings of National Heat Transfer Conference*, Vol. 2, ASME HTD-Vol. 96, 1988, pp. 405–408.
15. Wang, J. C. Y., Ma, Y. and Liu, J., Vapor condensation on a horizontal elliptical tube. *Proceedings of the XVIIIth International Congress of Refrigeration*, Paper No. 160, Montreal, Canada, 1991.
16. Yang, S. and Chen, C., Role of surface tension and ellipticity in laminar film condensation on a horizontal elliptical tube. *International Journal of Heat and Mass Transfer*, 1993, **36**(12), 3135–3141.
17. Fieg, G. P. and Roetzel, W., Calculation of laminar film condensation in/on inclined elliptical tubes. *International Journal of Heat and Mass Transfer*, 1994, **37**(4), 619–624.
18. Yang, S. and Chen, C., Laminar film condensation on a horizontal elliptical tube with variable wall temperature. *Journal of Heat Transfer*, 1994, **116**, 1046–1049.
19. Memory, S. B. and Rose, J. W., Free convection laminar film condensation on a horizontal tube with variable wall temperature. *International Journal of Heat and Mass Transfer*, 1991, **34**, 2775–2778.
20. Panday, P. K., Laminar film condensation of downward flowing vapour on a horizontal elliptical cylinder—a numerical solution. *International Communication on Heat and Mass Transfer*, 1987, **14**, 33–43.
21. White, F. M., *Viscous Fluid Flow*. McGraw-Hill, New York, 1974, pp. 256–257.
22. Crandall, S. H., *Engineering Analysis, A Survey of Numerical Procedures*. R. E. Krieger, 1986, pp. 174–187.
23. Gear, C. W., *Numerical Initial Value Problems in Ordinary Differential Equations*. Prentice-Hall, New Jersey, 1971, pp. 209–229.
24. Shigechi, T., Kawae, N., Tokita, Y. and Yamada, T., Film condensation heat transfer on a finite-size horizontal plate facing upward. *Heat Transfer—Japanese Research*, 1993, **22**, 66–77.
25. White, F. M., *Fluid Mechanics*, 2nd edn. McGraw-Hill, New York, 1986, p. 418.